Scripta Materialia 159 (2019) 68–71

Contents lists available at ScienceDirect

Scripta Materialia

journal homepage: www.elsevier.com/locate/scriptamat

Enhanced thermoelectric performance of Te-doped skutterudite with nano-micro-porous architecture

Houjiang Yang, Pengfei Wen *, Xilong Zhou, Yao Li, Bo Duan, Pengcheng Zhai *, Qingjie Zhang

Hubei Key Laboratory of Theory and Applications of Advanced Materials Mechanics, Wuhan University of Technology, Wuhan 430070, China

ARTICLE INFO

Article history:
Received 31 July 2018
Received in revised form 9 September 2018
Accepted 12 September 2018
Available online xxxx

Keywords:
Thermoelectric materials
Porous material
Thermal conductivity
Thermoelectric properties

ABSTRACT

Te-doped $Co_4Sb_{11.5}Te_{0.5}$ materials with nano to micro sized pores are fabricated tactfully by annealing the nano-$Co_4Sb_{11.5}Te_{0.5}$/$Co_4Sb_{11.5}Te_{0.5}$ composites. The annealed samples present a dramatically reduced thermal conductivity due to the abundant scattering of phonons in a wide wavelength range by the obtained all-scale porous architecture. Meanwhile, the Seebeck coefficient is enhanced for the annealed samples due to the lower carrier concentration. The sample annealed 100 h exhibits an enhanced dimensionless figure of merit of 1.2 at 800 K, increased by 33.7% as compared with that of the dense sample.

© 2018 Acta Materialia Inc. Published by Elsevier Ltd. All rights reserved.

Thermoelectric (TE) material that can directly and reversibly convert heat to electrical energy is attractive for its potential applications in power generation and cooling [1]. The efficiency of a TE material increases with the dimensionless figure of merit (ZT), defined as $\alpha^2\sigma T/\kappa$, where α is the Seebeck coefficient, σ is the electrical conductivity, T is the absolute temperature and κ is the thermal conductivity ($\kappa = \kappa_C + \kappa_L$, where κ_C is the carrier contribution and κ_L is the lattice contribution). Generally, two kinds of strategies have been developed to improve ZT, one is to maximize the power factor ($PF = \alpha^2\sigma$), the other is to suppress the κ.

Skutterudite $CoSb_3$ has attracted considerable attention in the past two decades because of its promising electrical performance in the intermediate temperature range. However, it displays a too high κ_L, which definitely hinders its practical applications [2]. To obtain a higher ZT, the κ_L should be further suppressed. Being the contribution due to phonons, κ_L can be greatly reduced by scattering the phonons by the different kinds of atomic [3,4], nano- [5,6], meso- [7,8] or micron-sized defects [9,10], the size of which is comparable to the mean free path (MFP) of heat-carrying phonons in skutterudite. Recently, a panoscopic approach has been presented [2,11–13], which can significantly reduce the κ_L by scattering phonons across multiple length scales.

Many studies suggested that introducing nano or micro size pores into TE materials was an effective method to reduce the κ_L [14–19]. Especially, Mori et al. reported that introducing nano-micropores through annealing co-doped $CoSb_3$ can lead to a striking enhancement of ZT [20]. However, in most previous studies, pores were often created by the evaporation of purposely added [9,16,17] or precipitated [10,20] volatile phase. Although, these additional phases can be removed by annealing, an accurate annealing time is always not easy to be grasped.

In this work, we present a facile method to fabricate a nano-micro-porous structure in $Co_4Sb_{11.5}Te_{0.5}$ materials via annealing the nano-$Co_4Sb_{11.5}Te_{0.5}$/$Co_4Sb_{11.5}Te_{0.5}$ composites, without introducing any additional phases. The structures and TE performance have been characterized in detail, and significant enhancement of ZT value has been achieved for the all-scale porous sample.

Co (99.9%), Sb (99.99%) and Te (99.9999%) powders with nominal composition of $Co_4Sb_{11.5}Te_{0.5}$ were well mixed, loaded into carbon crucibles, sealed in quartz tubes under vacuum and heated at 903 K for 50 h. The obtained ingots were ground into powders via a mortar and the fractional obtained powders were further grounded by ball milling (BM) at 250 rpm for 68 h under vacuum. The ball milled powders (10 wt%) and the powders without BM (90 wt%) were mixed, and then sintered by spark plasma sintering (SPS) under 50 MPa at 773 K for 7 min. The obtained bulk was named N10. Annealing treatments for the N10 was carried out at 773 K for 100 and 200 h in vacuum. The annealed samples were named as N10-A100 and N10-A200, respectively. For comparison, the bulk that did not incorporate ball milled powders was prepared by the same SPS process, which was named N0.

The phase purity was analyzed by X-ray diffraction (XRD, Bruker: D8 Advance, Cu Kα). The microstructures were examined by field-emission scanning electron microscopy (FESEM; Zeiss Ultra plus). The electrical conductivity σ and Seebeck coefficient α were measured synchronously by the standard four-probe method (Sinkuriko: ZEM-3). The Hall Coefficient R_H at 300 K was measured using a physical properties measurement system (PPMS, Quantum Design). The carrier concentration n and Hall mobility μ_H were calculated by using the relations $n = 1/(qR_H)$ and $\mu_H = \sigma R_H$, where q is the carrier charge. The thermal

---

* Corresponding authors.
E-mail addresses: pfwen@126.com (P. Wen), pczhai@126.com (P. Zhai).

https://doi.org/10.1016/j.scriptamat.2018.09.015
1359-6462/© 2018 Acta Materialia Inc. Published by Elsevier Ltd. All rights reserved.

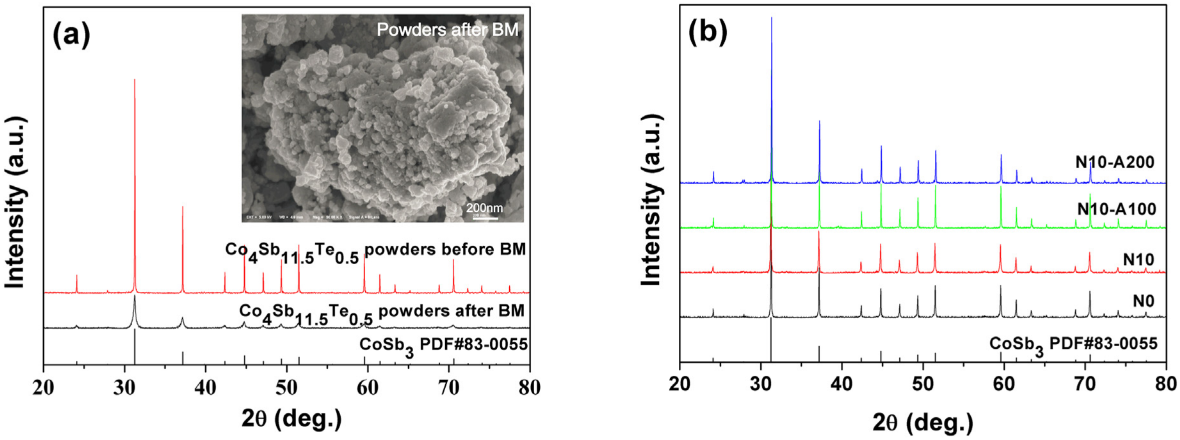

Fig. 1. (a) XRD patterns of $Co_4Sb_{11.5}Te_{0.5}$ powders before and after BM; (b) XRD patterns of bulks.

conductivity κ was calculated from the measured thermal diffusivity λ, heat capacity C_p, and density d by the relationship of $\kappa = C_p\lambda d$. Cp and λ were measured by the differential scanning calorimeter (TA: DSC Q20) and a laser-flash technique (Netzsch: LFA457), and d was measured with the Archimedes method. Uncertainties in σ and κ are ± 5%–7%. The uncertainty in α is ±5%.

Fig. 1(a) displays the XRD patterns of the $Co_4Sb_{11.5}Te_{0.5}$ powders before and after BM. All the diffraction peaks are well-matched with the standard PDF card of $CoSb_3$. The XRD peaks of the powders after BM exhibit a significant broadening and weakening, which is attributed to nanostructuring as well as a considerable amount of strain in the nanopowders [16]. The inset in Fig. 1(a) shows the FESEM image of the $Co_4Sb_{11.5}Te_{0.5}$ powders after BM, confirming that the powders after BM are composed of nanocrystals. Fig. 1(b) displays the XRD patterns of the bulk samples, which clearly shows that all the diffraction peaks are indexed to the single skutterudite phase.

Arrows, solid line circles and dash line circles mark the nano-particles, nano-scale pores and meso- to micro-scale pores, respectively.

Fig. 2 shows the FESEM images of the samples' fractured surfaces. It can be seen that the N0 sample possesses a dense structure, and the N10 contains not only the introduced nano-particles but some randomly distributed nanopores with sizes less than 200 nm. The formation of these nano-pores is probably caused by the release of the strain in the $Co_4Sb_{11.5}Te_{0.5}$ nano-particles during the sintering process. Compared with the N10, the N10-A100 has fewer nano-particles, but contains some irregularly shaped pores with sizes ranging from 200 nm to 2

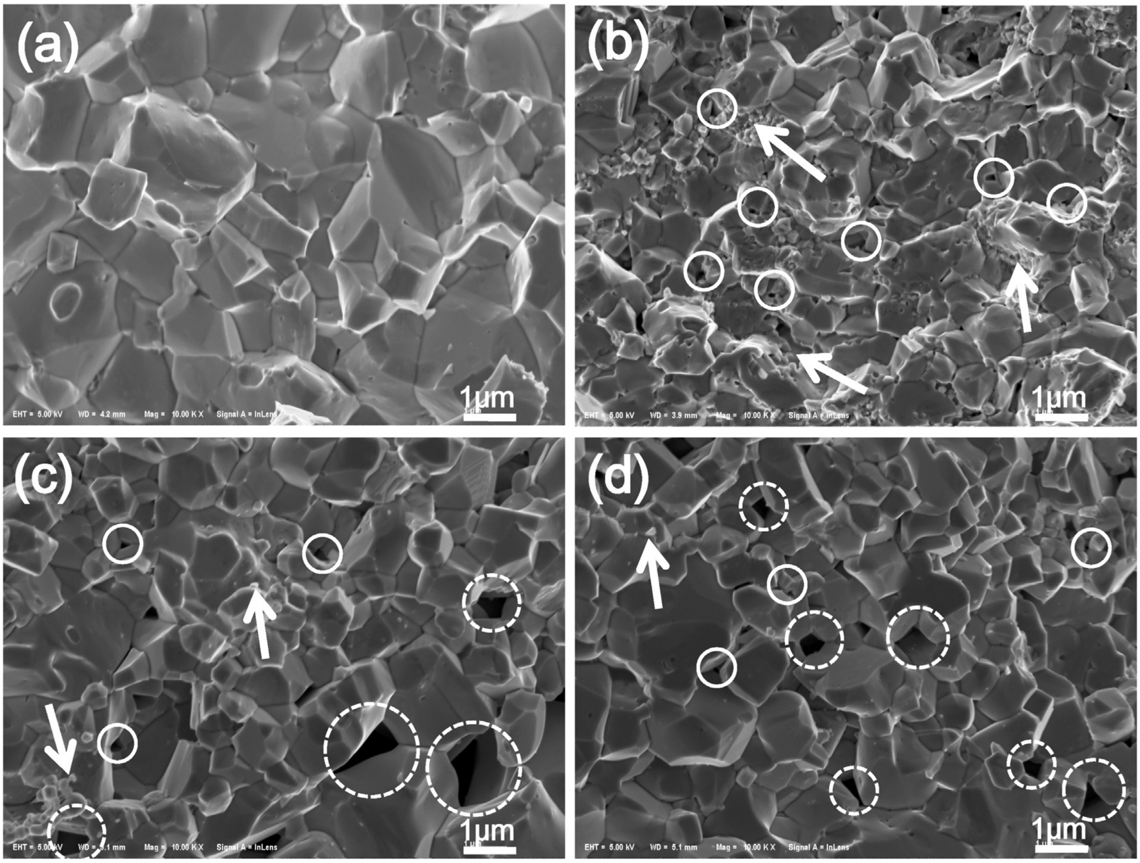

Fig. 2. FESEM images of fractured surfaces of the samples, (a) N0, (b) N10, (c) N10-A100 and (d) N10-A200.

Download English Version:

https://daneshyari.com/en/article/10147594

Download Persian Version:

https://daneshyari.com/article/10147594

Daneshyari.com